Yonsei Medical Journal
Vol. 40, No. 3, pp. 273−282, 1999

Ultrastructural Changes of the External Elastic Lamina in Experimental Hypercholesterolemic Porcine Coronary Arteries

Hyuck Moon Kwon, Seokmin Kang, Bum Kee Hong, Dongsoo Kim, Hyun Young Park, Mi Seung Shin, and Ki Hyun Byun

Abstract

The external elastic lamina (EEL) serves as a barrier for cells and macromolecules between the media and adventitia in the vascular wall. We evaluated the morphological changes and quantitative assessments of the EEL architecture in the coronary circulation of pigs fed with a high cholesterol diet. Confocal microscopy analysis of the EEL from hypercholesterolemic coronary arteries revealed an altered pattern characterized by fragmentation and disorganization of the EEL associated with an increase in the thickness. Computerized digital analysis of the images obtained by confocal scanning microscopy demonstrated that compared to normal coronary arteries, the EEL of hypercholesterolemic coronary arteries decreased in the percentage of their elastin content ($30.80 \pm 1.64\%$ vs. $47.85 \pm 1.82\%$, $p=0.001$). The percentage of elastin content was negatively correlated with the vessel wall area ($r=-0.82$, $p=0.001$). The immunoreactivity for matrix metalloproteinase-3 (MMP-3) increased in cholesterol-fed coronary arteries, predominantly in the neointima and adventitia. This study demonstrates that experimental hypercholesterolemia induced ultrastructural changes of the EEL in coronary circulation. The EEL may also be an atherosclerosis-prone area compared with the intima. The EEL may play an important role in the development of structural changes which characterizes the early phase of coronary atherosclerosis and vascular remodeling.

Key Words: Hyperchlolesterolemia, EEL, vascular remodeling, confocal microscopy, MMP-3

INTRODUCTION

The role of adventitia in vascular lesion formation has been largely ignored despite numerous studies which have suggested its potential importance.[1-4] However, adventitial reactions are common in atherosclerosis consisting of inflammation and fibrosis of the adventitia surrounding the EEL of diseased vessels.[3,4] More recent studies continue to indicate vascular remodeling of the human atherosclerotic coronary artery.[5,6] Furthermore, vascular remodeling, as indicated by a change of the EEL after angioplasty, may contribute to restenosis.[7] In a chronic atherosclerotic process, these adaptive geometric changes may mediate myofibroblast-dependent extracellular matrix reorganization.[8]

Several studies have demonstrated discontinuities and abnormalities in the internal elastic lamina (IEL) structure of elastic and muscular arteries during advanced atherosclerosis.[9-15] It has been hypothesized that structural defects in the IEL may play an important role during the formation of an atherosclerotic lesion, allowing cell migration and macromolecule transfer between the intima and different layers of the vascular wall.[10,14] There is a lack of information regarding the ultrastructural changes of the EEL in coronary artery diseases. Furthermore, it is not known whether this process is also taking place in the EEL at an early stage of atherosclerosis.

The present study is the first to provide quantitative data comparing elastin content and metalloproteinase activity in experimental hypercholesterolemic porcine coronary arteries. Since experimental hypercholesterolemia is characterized by structural and functional changes in coronary arteries which resemble those present in the early phase of coronary ather-

Received April 8, 1999
Accepted May 13, 1999
Cardiology Division, Department of Internal Medicine, Yonsei University College of Medicine, Seoul, Korea
This study was supported by a research grant of Yonsei University College of Medicine for 1998.
Address reprint request to Dr. H. M. Kwon, Department of Internal Medicine, Yongdong Severance Hospital, Yonsei University College of Medicine, Yongdong P.O. Box 1217, Seoul 135-270, Korea. Tel: 82-2-3497-3330, Fax: 82-2-573-0112, E-mail: hmkwon@yumc.yonsei.ac.kr

osclerotic development,[16] we therefore designed this study to evaluate the ultrastructural appearance of the EEL in porcine coronary arteries treated with a high cholesterol diet. By the use of confocal microscopy,[17] it was possible to visualize the ultrastructure of the EEL and to evaluate the presence of morphological changes both qualitatively and quantitatively using a computerized digital imaging analysis technique.

MATERIALS AND METHODS

Arterial specimens

The experiments were performed using 9 female juvenile domestic crossbred pigs weighing 25−35 kg. Five pigs were placed on a normal laboratory chow diet (Group 1). Another 4 animals were fed with a high-cholesterol diet consisting of 2% cholesterol and 15% lard by weight (TD 93296, Harlan Tekiad) for 10 to 12 weeks (Group 2). Plasma total cholesterol and lipoprotein levels were determined by an enzymatic method previously described,[18] using a commercial reagent (Roche Research Foundation, Basel, Switzerland). At the time of sacrifice, after plasma cholesterol level measurements, the animals were euthanized using 10 ml of an intravenous commercial euthanasia solution (Sleepaway, Fort Dodge Lab., Fort Dodge, IA, USA) by the ear vein.

Tissue preparation and histochemistry

Immediately following removal of the heart, each heart was placed on a fixation pump and perfused with 10% Formalin at 70 mmHg of pressure to maintain coronary artery morphologic integrity. Twelve coronary segments (4 left anterior descending, 4 left circumflex, and 4 right coronary arteries) from the hypercholesterolemic group and 15 segments (5 left anterior descending, 5 left circumflex, and 5 right coronary arteries) from the control group were evaluated. To preserve the integrity of the adventitia and perivascular tissues, the porcine coronary arteries were carefully removed in a segment along with adjacent tissues (i.e., adipose tissue, myocardium) and rinsed with phosphate buffered saline (PBS). Then each coronary segment harvested from the proximal or midportion of the coronary artery was cut transversely into three specimens of 2−3 mm in length. The specimen corresponding to the proximal part of the coronary segment and the specimen corresponding to the distal part of the coronary segment were excluded from the analysis to avoid artifacts due to segment manipulation.

Each segment was embedded in paraffin and cut in 5 m sections, which were stained with hematoxylin-eosin (H & E) and elastic van Giesion stains. By computerized morphometric analysis (JAVA, Jandel Scientific Co., Corte Madera, CA, USA) the following morphometric variables were measured: (a) intimal thickness; (b) EEL thickness, defined as between the inner and outer EEL border; (c) adventitia thickness, defined as between the perivascular adipose tissue and EEL; and (d) vessel wall area, defined as the area circumscribed by the outer EEL. Elastic van Giesion-stained cross sections were used for morphometric measurements of intimal thickness using a magnification of 4x. The thickness of the intimal layer (defined as the distance from the lumen surface of the endothelium to the inner border of the IEL) was manually traced at 8 different sites around the entire circumference of the vessel wall. A mean value was obtained for each coronary segment.

Confocal microscopy

Confocal microscopy was utilized for the identification of elastic fibers in the H & E staining of porcine coronary arteries. The fluorescent properties of stained elastic fibers were due to eosin staining as revealed by fluorescence analysis of the dye in solution, with a negligible or only minor contribution by elastin auto-fluorescence.[17,19] H & E-stained coronary arteries were also used for comparison with light microscopic histologic architecture and morphological examination of elastin patterns under the confocal microscope, using the corresponding sections (Fig. 1).[19,20] Experiments were performed in duplicate and analyzed on a confocal laser scanning microscope LMS 310 (Carl Zeiss Inc., Oberkochen, Germany) equipped with an argon/krypton laser. The elastic laminae of the coronary artery were visible by means of their autofluorescence with the laser tuned to an excitation wave length of 488/568 nm and the emissions collected through a 530/20 nm band-pass filter (pinhole =20). Images per specimen (hypercholesterolemic group, total number of fields=20; control group, n=20) were examined using a 10× neofluor lens with 0.3

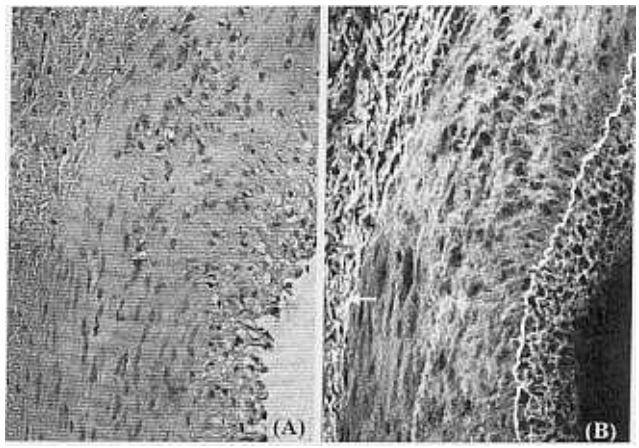

Fig. 1. H & E staining (Panel A, final magnification 320 ×) and laser scanning confocal microscopy of the coronary artery (Panel B, magnification 320 ×) from a hypercholesterolemic animal. In hypercholesterolemic animals, the EEL (white arrow) appeared irregular and disorganized, which was associated with thickening of the EEL. Foam-cell infiltration of the thickened subendothelium was seen mainly in the intima, which was associated with internal elastic lamina fragmentation.

n.a., digitized with a matrix of 512×512 pixels with a resolution of 1.25 μm per pixel and a field size of 0.4096 mm^2.

Furthermore, in order to digitally quantitate the average thickness and elastin content of the EEL, corresponding images were examined using a 40× neofluor lens with 0.75 n.a., digitized with a matrix of 512×512 pixels at a resolution of 0.625 μm per pixel and a field size of 0.1024 mm^2. An image of the elastic laminae was stored using the LSM 310 software on an IBM work station. Control experiments were performed under the same conditions. The results were analyzed independently by two analysts who were blinded to the diet regimen.

Digital image analysis and quantification of elastin content

The overlaid elastic laminae images obtained by confocal microscopy were captured and digitized on a computer station (Sun Microcomputer, Corte Madera, CA, USA). Quantitative morphometric measurements of the elastic laminae were obtained using the Analyze Software (Version 7.5, Biomedical Imaging Resource, Mayo Foundation, Rochester, MN, USA). Average elastin content of the EEL was calculated respectively. The measurements were obtained as follows: a region of interest (ROI) was manually traced of the inner and outer EEL, excluding the medial and adventitia amorphous elastin content. Then an intensity histogram was selected, displaying the occurrence of gray levels (from white to black) within the ROI. Each elastic lamina area (displayed in white) was differentiated against the black background, which represented the elastin fibers, by setting the lower threshold values for an intensity range of interest (IROI) that yielded the best identification of autofluorescent elastic laminae regions as judged by the analyst (Fig. 1). The number of pixels that composed the area surrounded by the elastic fibers was then automatically counted by the computer. The values were divided by the total number of pixels within the image to obtain a percentage of the elastin content of the EEL.

The thickness of the EEL layer (defined as the distance from the innermost to outermost border of the EEL) was manually traced at 8 different sites around the entire circumference of the vessel wall. A mean value was obtained for each coronary segment.

Immunohistochemistry for MMP-3

Paraffin sections (5 μm) were made and transferred to glass slides. The slides were deparaffinized and rehydrated through the following solutions: xylene twice for 5 minutes, 100% ethanol twice for 10 dips and 95% ethanol twice for 10 dips. Endogenous peroxidase activity was blocked for 10 minutes at room temperature in 50% volume H_2O_2/50% volume methanol and rinsed in running tap water. Non-specific protein binding sites were blocked by applying 5% normal goat serum diluted in PBS/0.05% Tween 20 (pH=7.2−7.4) to slides for 10 minutes at room temperature. The serum was blotted off and the primary antibody (rabbit polyclonal antibodies for MMP-3, Merck Research Foundation, Whitehouse Station, NJ, USA) was diluted in 1% normal goat serum & PBS/0.05% Tween 20, applied and incubated overnight at 4°C in a humidity chamber. On day 2, the primary antibody was rinsed off in tap water, blotted and the biotinylated secondary antisera cocktail, including goat anti-mouse IgG and goat anti-rabbit IgG diluted 1/400, was incubated on the slides for 30 minutes at room temperature. The slides were rinsed in running tap water, blotted and then a mixture of streptavidin-horseradish peroxidase diluted 1/500 in PBS/0.05% Tween 20 and 1% normal goat serum were applied

and the slides were incubated for 30 minutes at room temperature. The slides were rinsed in tap water and color developed in 3-amino-9-ethylcarbazole substrate solution for 15 minutes at room temperature, then counterstained in hematoxyline for 30 seconds and covered with coverslip.

Stock Solutions

Tween 20 (Pierce Chemical, Rockford, Ill, USA)
Normal goat serum (Dako, Carpinteria, CA, USA)
Biotinylated mouse IgG (Dako, Carpinteria, CA, USA)
Biotinylated rabbit IgG (Dako, Carpinteria, CA, USA)
Streptavidin-horseradish peroxidase (Dako, Carpinteria, CA, USA)
3-amino-9-ethycarbasole (Sigma, St. Louis, MO, USA)

Statistical analysis

Differences between groups in the plasma cholesterol values and in the morphometric measurements were assessed by a one-way ANOVA test followed by Mann-Whitney U-Wilcoxon Rank Sum W test. Linear regression analysis was utilized to evaluate the relationship between elastin content and morphometric measurements. A value of $p<0.05$ was considered significant in all analyses. All data in the text and figures were presented as mean±standard error.

RESULTS

A significant increase in plasma cholesterol and low-density lipoprotein was present in the group of animals fed with a high cholesterol diet compared with the control group (Table 1).

Compared with control coronary arteries, the increase in cellularity of the adventitia accompanied the infiltration of inflammatory cells, such as foam cells (Fig. 2). Control coronary arteries revealed little MMP-3 immunoreactivity (Fig. 3A). Hypercholesterolemic coronary arteries demonstrated marked increases in MMP-3 immunoreactivity, predominantly in the thickened intima and the adventitia. MMP-3 immunoreactivity in the intima and adventitia was distributed within multi-layered elastic laminae (Fig. 3B).

Histomorphometric analysis demonstrated a significant difference in the intimal thickness between controls and hypercholesterolemic coronary arteries (7.85 ±0.53 μm vs. 120.75±10.20 μm, p=0.001) (Fig. 4A). Confocal microscopy analysis of the coronary arteries from control pigs demonstrated that the EEL was smooth and regular without disruption of its structure (Fig. 5, A and C). Conversely, the EEL from hypercholesterolemic coronary arteries revealed an altered pattern characterized by fragmentation and disorganization of the EEL associated with an increase in the thickness (90.78±4.12 μm vs. 215.77±13.20 μm, respectively; p=0.001) (Fig. 4B, 5, B and D). As depicted in figure 5B and 5D, the most striking changes in peri-adventitial dimension were present in the regions adjacent to the site of the EEL. Adventitial thickness was almost doubled compared with the EEL thickness (187.57±9.52 μm vs. 428.77± 15.40 μm) (Fig. 4C), suggesting that the adventitial thickening accompanied the EEL thickening. Elastin fibers in the EEL of hypercholesterolemic animals were globular in form and loosely packed, and were sometimes aligned radially in the vessel wall (Fig. 5D). High-magnification views of H & E - stained sections

Table 1. Lipid Profile and Morphometric Data in the Two Experimental Groups

	Control (n=20)	Hypercholesterolemia (n=20)
Cholesterol (mg/dl)	106±11	341±75*
Low density lipoproteins (mg/dl)	34±20	263±72*
High density lipoproteins (mg/dl)	33±2	71±6*
Intimal thickness (μm)	7.85±0.53	120.75±10.20*
Adventitial thickness (μm)	187.57±9.52	428.77±15.40*
EEL thickness (μm)	90.78±4.12	215.77±13.20*
Percent elastin content of EEL (%)	47.85±1.82	30.80±1.64*
Vessel wall area (mm^2)	5.75±0.14	8.28±0.27*

EEL, external elastic lamina.
*$p<0.05$.

showed increased cellularity among the loose fibers in the EEL of hypercholesterolemic coronary arteries, which suggested fragmentation and disorganization (Fig. 2B and 5D). Normal elastin fibers were replaced with amorphous elastin and collagen materials (Fig. 5, A and B).

Computerized digital analysis of the images obtained by confocal scanning microscopy demonstrated that compared to normal coronary arteries, the EEL of hypercholesterolemic coronary arteries decreased in the percentage of their elastin content (30.80±1.64% vs. 47.85±1.82%, p=0.001) (Fig. 6A). There was a negative correlation between the vessel wall area and the percentage of elastin content (r=−0.82, p=0.001) (Fig. 6B).

DISCUSSION

This study demonstrated that in porcine coronary circulation, experimental hypercholesterolemia is asso-

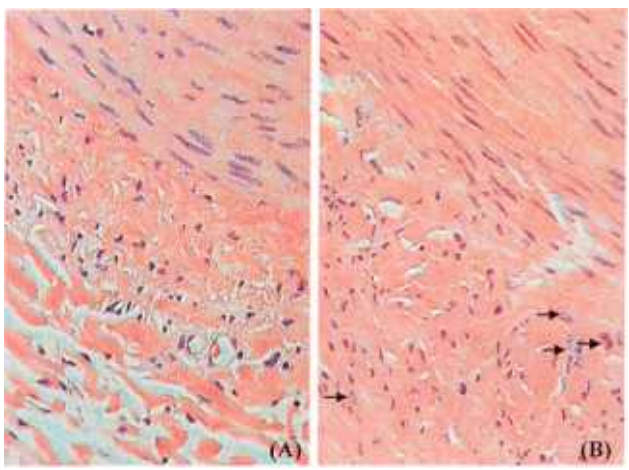

Fig. 2. H & E stained micrographs in a normal (Panel A, final magnification 400×) and a cholesterol-fed (Panel B, final magnification 400×) porcine coronary artery. The cholesterol-fed coronary artery demonstrated a marked increase in cellularity, predominantly in the adventitia and outer media. Within the hypercholesterolemic coronary artery specimen, the foam-cells were evident in the adventitia and outer media (black arrows).

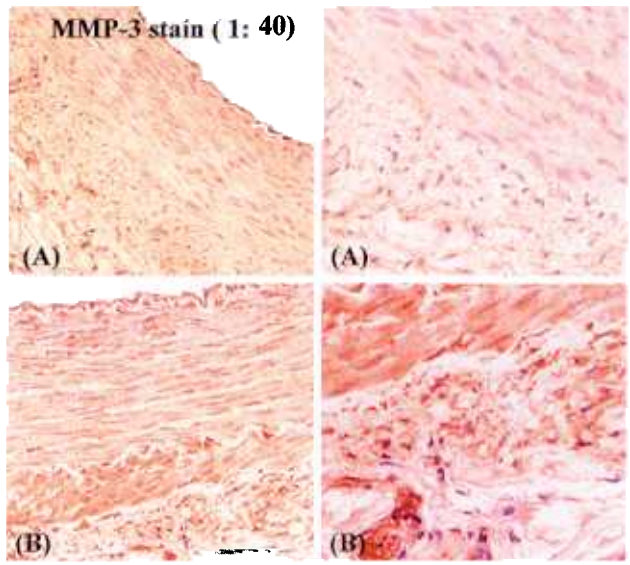

Fig. 3. Immunohistochemical demonstration of MMP-3 in normal (Panel A, final magnification 200× & 400×) and hypercholesterolemic (Panel B) coronary arteries. The hypercholesterolemic coronary artery demonstrated a marked increase in MMP-3 immunoreactivity, predominantly in the EEL and adventitia.

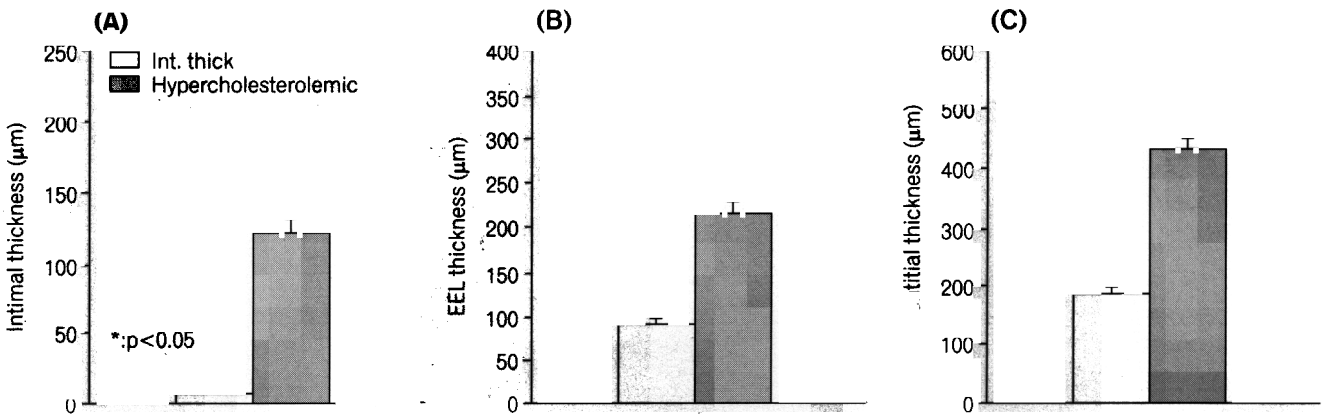

Fig. 4. Morphometric measurements obtained by H & E - stained microscopy images. Significant differences were observed in the intimal thickness (Panel A), the EEL thickness (Panel B) and the adventitial thickness (Panel C) between hypercholsterolemic and control animals.

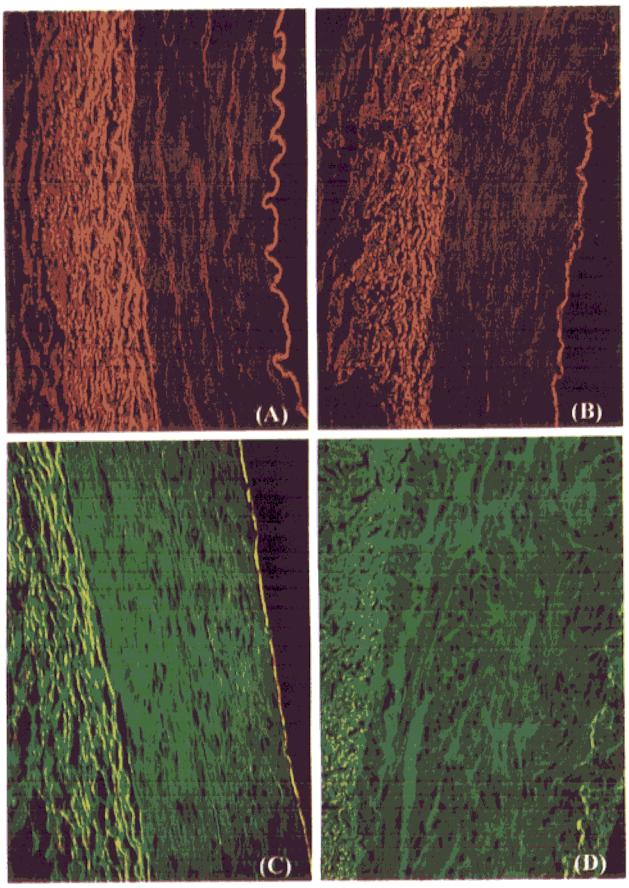

Fig. 5. Laser scanning confocal microscopic images of the IEL from a control (Panel A & C, final magnification 320×) and hypercholesterolemic animal (Panel B & D). Laser scanning confocal micrography in hypercholesterolemic coronary EEL revealed that the elastic lamina was fragmented and widened by elastolytic activity and thickening of the EEL. The most striking changes in peri-adventitial dimension were present in the regions adjacent to the site of the EEL.

ciated with significant morphological and ultrastructural changes of the EEL. These changes were characterized by fragmentation and disorganization of the EEL associated with an increase in the thickness. The decrease in the percentage of their elastin content in the EEL was associated with elastolytic activity. The immunoreactivity for MMP-3 increased in cholesterol-fed coronary arteries, predominantly in the thickened intima and adventitia. The percentage of elastin content was negatively correlated with the vessel wall area. This EEL change may be associated with the neoadventitial formation and phenotypic change of myofibroblasts. The present study suggests that ultrastructural changes of the EEL may play an important role in the development of atherosclerotic matrix reorganization and vascular remodeling. The arterial wall is an integrated functional component of the circulatory system that is continually remodeling in response to hemodynamic conditions and disease states. The present study focused on the ultrastructure of EEL in the coronary arteries in a porcine model of experimental hypercholesterolemia and utilized for the first time the laser scanning confocal microscopy technique to visualize the ultrastructure of the EEL.[17] In addition, this method allowed us to assess the ultrastructural changes of the EEL both qualitatively and quantitatively using a computerized digital imaging analysis system.[11,19]

The role of adventitia in vascular lesion formation has been largely ignored despite numerous studies that have suggested its potential importance. Adven-

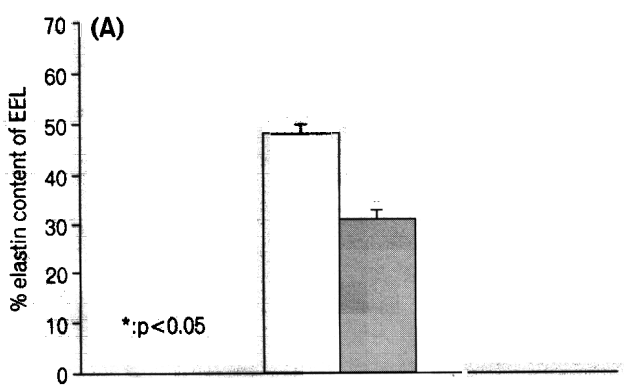

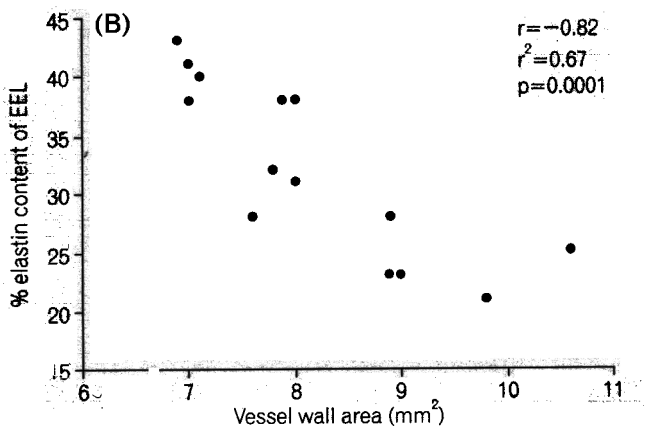

Fig. 6. Quantitative digital analysis of corresponding images obtained by H & E staining and confocal microscopy demonstrated a statistically significant decrease of the elastin content in hypercholesterolemic coronary arteries, predominantly in the EEL, compared with normal coronary arteries (47.85±1.82% vs. 30.80±1.64%, $p<0.05$, Panel A). Panel B shows the correlation between the percentage of elastin content and the vessel wall area in corresponding coronary segments of hypercholesterolemic animals (closed circle).

titial inflammation is common in experimental studies of hypercholesterolemia in monkeys and pigs. Advanced lesions in these animals are also associated with an intense adventitial inflammation. Together, these studies suggested that adventitial inflammation may occur early in the atherosclerotic process and may precede or be coincident with the invasion of mononuclear cells into the arterial intima.[2-4] The mechanisms underlying adventitial inflammation and reaction during atherosclerotic lesion development are not yet understood. Elevated lipids may play a role in initiating atherosclerotic lesion development by stimulating inflammatory cytokine production, which may in turn initiate the inflammatory process. Inflammatory cytokines were localized to macrophages and endothelial cells overlying atherosclerotic lesions. Minimally oxidized LDL and beta-VLDL upregulate inflammatory cytokines, thereby attracting more leukocytes to develop atherosclerotic plaque, beginning the cycle of inflammation and intimal development.[21,22] As well, oxidized LDL and vascular endothelial growth factor (VEGF) accumulated in human atherosclerotic lesions induces the production of macrophage VEGF.[23] Also, VEGF upregulates the expression of matrix metalloproteinases in vascular smooth muscle cells.[24] Similar events may occur in the adventitia during atherosclerotic development where the adventitial vasa vasorum endothelial cells may be affected by elevated lipids and express adhesion molecules early in the atherosclerotic process, thus contributing to the invasion of inflammatory cells into the adventitia as well.[21,22,25] Experimental hypercholesterolemia may induce the upregulation of specific cell-surface receptors in the adventitial vasa vasorum, which then predisposes them to proliferate in response to growth factors and an increase in the vessel wall thickness.[26-28] Recently, Jamieson and co-authors have demonstrated a correlation between apo(a) deposition within endothelial cells of vasa vasorum and the stage of atherosclerotic plaque, suggesting a specific link between apo(a) receptor and the pathogenesis of atherosclerosis.[29] Specifically, it has been demonstrated that the low-density lipoprotein receptor-related protein/α_2-macroglobulin receptor, which is present normally in endothelial cells of the adventitial vasa vasorum and smooth muscle cells of the media, may play an important local scavenger role for certain cytokine/growth factors.[30-32]

Then thread stimulated a local inflammatory response in the adventitia, eventually resulting in the ultrastructural changes of the EEL. Furthermore, there is considerable evidence suggesting that a wide range of cellular components of normal and diseased vessel walls, such as smooth muscle cells, macrophages, and fibroblasts, can degrade the extracellular matrix. Of particular interest, it has been shown that vascular smooth muscle cells are capable of producing enzymes that will degrade both basement membranes and the extracellular matrix.[33] In vitro models have been used to demonstrate MMP-3 gene expression in response to mechanical injury in vascular smooth muscle cells.[34] Recently, several experimental studies have shown that in response to an increased presence of mildly oxidized lipoproteins in the outer media,[35] which have been shown to be chemotactic for monocytes,[36] an increased number of monocytes can enter the intima and adventitia under hypercholesterolemic conditions.[37] Different studies have shown by in situ zymography and in situ hybridization that there is an expression of MMP-3 in adventitial macrophages of atherosclerotic vessels.[33,38,39] In particular, mRNA transcripts for MMP-3 have been localized into smooth muscle cells and macrophage foam cells both in fibrous and lipid-rich atherosclerotic lesions.[39-43] In addition, studies using immunoprecipitation to examine human abdominal aortic aneurysm specimens have shown high levels of MMP localized to the vasa vasorum, which may be involved in matrix remodeling.[44] Since the lesions in experimental hypercholesterolemia resemble those present in human atherosclerosis, it may be speculated that an increased production and release of metalloproteinase in the outer media and the adventitia may mediate the pathologic ultrastructural changes of the EEL in this model. MMP-3 degrades proteoglycan core proteins, fibronectin, collagen, laminin, and gelatin and can activate other MMPs. MMP-3 digestion of proteoglycan core proteins can thereby enhance subsequent elastin degradation.[40,43,45,46] MMP-3 activity, the net elastolytic activity, induced the ultrastructural changes in the EEL of hypercholesterolemic coronary arteries. Such a disruption of elastin is enough to facilitate the migration of myofibroblasts and the proliferation of smooth muscle. Thus, elastin is a molecular determinant of arterial morphogenesis such as vascular remodeling, stabilizing arterial structure by regulating proliferation and reorganization of vascular smooth muscle.[47] Our finding is in agreement with these observations,

since infiltration of inflammatory cells in the adventitia was frequently found during histologic study. The decrease in the percentage of elastin content in the EEL was associated with elastolytic activity. The immunoreactivity for MMP-3 increased in cholesterol-fed coronary arteries, predominantly in the thickened intima and adventitia. The percentage of elastin content was negatively correlated with the vessel wall area. This EEL change may be associated with the vascular geometric remodeling and phenotypic change of myofibroblasts. This study suggests that ultrastructural changes of EEL may play an important role in the development of matrix reorganization, resulting in vascular remodeling.

Arterial remodeling is well described in de novo atherosclerosis.[5,6,48] Studies by others[49-52] have also demonstrated that abnormal geometric remodeling of a vessel is the primary determinant of restenosis in the atherosclerotic model. We showed that the enlargement of the vessel wall area is associated with an increase in the EEL thickness and a decrease in the percentage of the elastin content of the EEL in an experimental hypercholesterolemic porcine model, irrespective of the degree of intimal hyperplasia. Contrary to collagen, elastin has an extremely long half-life (40−70 years). Loss of elastin is almost certainly a manifestation of excessive elastolysis rather than insufficient synthesis. In light of the findings in this study, that the elastin content of the hypercholesterolemic coronary artery was lower than that of the normal coronary artery and that the percentage of elastin content was negatively correlated with the vessel wall area in a noninjured hypercholesterolemic model was due to favorable remodeling, it is reasonable to strongly suspect that elastolytic activity or the resultant increased collagen-to-elastin ratio of the EEL plays an important role in vascular remodeling. However, the mechanisms of remodeling are poorly understood,[53] and a causal relationship between adaptive compensatory enlargement and elastin content in the EEL has not been established. Recently, animal experimental study demonstrated that arterial remodeling, occurring as the accumulation of intimal and medial mass, was correlated with expansion of the EEL following coronary angioplasty.[54]

The objective of this study was to examine the morphological ultrastructural changes in the EEL during experimental hypercholesterolemia. An improved understanding of the molecular mechanisms between the cell-extracellular matrix involved in atherogenesis and the progression of this disease is likely to yield new therapeutic strategies against this potentially lethal disease. Fragmentation and disorganization of the EEL may contribute to change vascular geometric remodeling. Further studies are needed to better understand the functional significance of the adventitial elastin that characterizes the EEL of coronary arteries in the early phase of atherosclerotic lesion formation.

REFERENCES

1. Horn H, Finkelstein LE. Arteriosclerosis of the coronary arteries and the mechanism of their occlusion. Am Heart J 1940;19:655-82.
2. Gerlis LM. The significance of adventitial infiltrations in coronary atherosclerosis. Br Heart J 1956;18:166-72.
3. Schwartz CJ, Mitchell JRA. Cellular infiltration of the human arterial adventitia associated with atheromatous plaques. Circulation 1962;26:73-8.
4. Wilcox JN, Scott NA. Potential role of the adventitia in arteritis and atherosclerosis. Int J Cardiol 1996;54:S21-35.
5. Glagov S, Weisenberg E, Zarins CK, Stankunavicius R, Kolettis GJ. Compensatory enlargement of human atherosclerotic coronary arteries. N Engl J Med 1987;316:1371-5.
6. Hermiller JB, Tenaglia AN, Kisslo KB. In vivo validation of compensatory enlargement of atherosclerotic coronary arteries. Am J Cardiol 1993;71:665-8.
7. Post MJ, Borst C, Kuntz RE. The relative importance of arterial remodeling compared with intimal hyperplasia in lumen renarrowing after balloon angioplasty: a study in the normal rabbit and the hypercholesterolemic Yucatan micropig. Circulation 1994;89:2816-21.
8. Shi Y, O'Brien JE, Ala-Kokko L, Chung W, Mannion JD, Zalewski A. Origin of extracellular matrix synthesis during coronary repair. Circulation 1997;95:997-1006.
9. Nakatake J, Wasano K, Yamamoto T. Three-dimensional architecture of elastic tissue in early arteriosclerotic lesions of rat aorta. Atherosclerosis 1985;57:199-208.
10. Sims FH. Discontinuities in the internal elastic lamina; a comparison of coronary and internal mammary arteries. Artery 1985;13:127-43.
11. Nakatake J, Yamamoto T. Three-dimensional architecture of elastic tissue in athero-arteriosclerotic lesions of the rat aorta. Atherosclerosis 1987;64:191-200.
12. Roach MR, Song SH. Arterial elastin as seen with scanning electron microscopy: a review. Scanning Microscopy 1988;2:993-1004.
13. Martin BJ, Stehbens WE, Davis PF, Ryan PA. Scanning electron microscopic study of hemodynamically induced tears in the internal elastic lamina of rabbits arteries. Pathology 1989;21:207-12.

14. Sims FH, Gavin JB, Vanderwee MA. The intima of human coronary arteries. Am Heart J 1989;118:32-8.
15. Rekhter MD, Andreeva ER, Mironov AA, Orekhov AN. Three-dimensional cytoarchitecture of normal and atherosclerotic intima of human aorta. Am J Pathol 1991;138: 569-80.
16. Kockx MM, DeMeyer GR, Bortier H, DeMeyer N, Muhring J, Bakker A, et al. Luminal foam cell accumulation is associated with smooth muscle cell death in the intimal thickening of human saphenous vein grafts. Circulation 1996;94:1255-62.
17. Wong LCY, Langille BL. Development remodeling of the internal elastic lamina of rabbit arteries. Circ Res 1996;78: 799-805.
18. Allain CC, Poon LS, Chan CSL, Richmond W, Fu PC. Enzymatic determination of total serum cholesterol. Clin Chem 1974;20:470-5.
19. De Carvalho HF, Toboga SR. Fluorescence and confocal laser scanning microscopy imaging of elastic fibers in hematoxylin-eosin stained sections. Histochem Cell Biol 1996;106:587-92.
20. Jester JV, Andrews PM, Petroll WM, Lemp MA, Cavanagh HD. In vivo, real-time confocal imaging. J Electron Micro Tech 1991;18:50-6.
21. Berliner JA, Territo MC, Sevanian A, Ramin S, Kim JA, Bamshad B, et al. Minimally modified low density lipoprotein stimulates monocyte endothelial interactions. J Clin Invest 1990;85:1260-6.
22. Wilcox JN, Nelken NA, Coughlin SR, Gordon D, Schall TJ. Local expression of inflammatory cytokines in human atherosclerotic plaques. J Athero Thromb 1995;1:S10-3.
23. Ramos MA, Kuzuya M, Esaki T, Miura S, Satake S, Asai T, et al. Induction of macrophage VEGF in response to oxidized LDL and VEGF accumulation in human atherosclerotic lesions. Arterioscler Thromb Vasc Biol 1998;18: 1188-96.
24. Wang H, Keiser JA. Vascular endothelial growth factor upregulates the expression of matrix metalloproteinases in vascular smooth muscle cells. Circ Res 1998;83:832-40.
25. Wood KM, Cadogan MD, Ramshaw AL, Parums DV. The distribution of adhesion molecules in human atherosclerosis. Histopathology 1993;22:437-44.
26. Edelman ER, Nugent MA, Smith LT, Karnovsky MJ. Basic fibroblast growth factor enhances the coupling of intimal hyperplasia and proliferation of vasa vasorum in injured rat arteries. J Clin Invest 1992;89:465-73.
27. Isner JF. Vasa vasorum; Therapeutic implications. Cathet Cardiovasc Diagn 1996;39:221-3.
28. Kwon HM, Sangiorgi G, Ritman EL, McKenna C, Holmes DR, Schwartz RS, et al. Enhanced coronary vasa vasorum neovascularization in experimental hypercholesterolemia. J Clin Invest 1998;101:1551-6.
29. Jamieson DG, Usher DC, Radier DJ, Lavi E. Apolipoprotein(a) deposition in atherosclerotic plaques of cerebral vessels; a potential role for endothelial cells in lesion formation. Am J Pathol 1995;147:1567-74.
30. San-Huang J. α_2-macroglobulins; a modulator for growth factors. Am J Respir Cell Mol Biol 1989;1:169-70.
31. James K. Interactions between cytokines and α_2-macroglobulin. Immunol Today 1990;11:163-6.
32. Lupu F, Heim D, Bachmann F, Kruithof EKO. Expression of LDL receptor-related protein/α_2-macroglobulin receptor in human normal and atherosclerotic arteries. Arterioscler Thromb 1994;14:1438-44.
33. Galis ZS, Muszynski M, Sukhova GK, Simon-Morrissey E, Unemori EN, Lark MW, et al. Cytokine-stimulated human vascular smooth muscle cells synthesize a complement of enzymes required for extracellular matrix digestion. Circ Res 1994;75:181-9.
34. James TW, Wagner R, White LA, Zwolak RM, Brinkerhoff CE. Induction of collagenase and stromelysin gene expression by mechanical injury in vascular smooth muscle-derived cell line. J Cell Physiol 1993;157:426-37.
35. Juul K, Nielsen LB, Munkholm K, Stender S, Nordestgaard BG. Oxidation of plasma low-density lipoprotein accelerates its accumulation and degradation in the arterial wall in vivo. Circulation 1996;94:1698-704.
36. Quinn MT, Parthasarathy S, Fong LG, Steinberg D. Oxidatively modified low density lipoproteins; a potential role in recruitment and retention of monocyte/macrophages during atherogenesis. Proc Natl Acad Sci USA 1987;84: 2995-8.
37. Lewis JC, Taylor RG, Jerome WG. Foam cell characteristics in coronary arteries and aortas of white carneau pigeons with moderate hypercholesterolemia. Ann NY Acad Sci 1985;454:91-100.
38. Henney AM, Wakeley PR, Davies MJ, Foster K, Hembry R, Murphy G, et al. Localization of stromelysin gene expression in atherosclerotic plaques by in situ hybridization. Proc Natl Acad Sci USA 1991;88:8154-8.
39. Dollery CM, McEwan JR, Henney AM. Matrix metalloproteinases and cardiovascular disease. Circ Res 1995;77: 863-8.
40. Newman KM, Ogata Y, Malon AM, Irizarry E, Gandhi RH, Nagese H, et al. Identification of matrix metalloproteinases 3(stromelysin-1) and 9(gelatinase B) in abdominal aortic aneurysm. Arteriosclerosis 1994;14:1315-20.
41. Pauly RR, Passaniti A, Bilato C, Monticone R, Cheng L, Papadopoulos N, et al. Migration of cultured vascular smooth muscle cells through a basement membrane barrier requires type 4 collagenase activity and is inhibited by cellular differentiation. Circ Res 1994;75:41-54.
42. Strauss BH, Robinson R, Batchelor WB, Chisholm RJ, Ravi G, Natarajan MK, et al. In vivo collagen turnover following experimental balloon angioplasty injury and the role of matrix metalloproteinases. Circ Res 1996;79:541-50.
43. Knox JB, Sukhova GK, Whittemore AD, Libby P. Evidence for altered balance between matrix metalloproteinases and their inhibitors in human aortic diseases. Circulation 1997;95:205-12.
44. Herron GS, Unemori E, Wong M, Rapp JH, Hibbs MH, Stoney RJ. Connective tissue proteinases and inhibitors in abdominal aortic aneurysms. Arterioscler Thromb 1991; 11:1667-77.
45. Jones PA, Werb Z. Degradation of connective tissue mat-

rices by macrophages; influence of matrix composition on proteolysis of glycoproteins, elastin, and collagen by macrophages in culture. J Exp Med 1980;152:1527-33.
46. Oho S, Rabinovitch M. Post-cardiac transplant arteriopathy in piglets is associated with fragmentation of elastin and increased activity of a serine elastase. Am J Pathol 1994;145:202-10.
47. Li DY, Brook B, Davis EC, Mecham RP, Sorensen LK, Boak BB, et al. Elastin is essential determinant of arterial morphogenesis. Nature 1998;393:276-90.
48. Zarin CK, Weisenberg E, Koettis G, Stankunavicius R, Glagov S. Differential enlargement of artery segments in response to enlarging atherosclerotic plaques. J Vasc Surg 1988;7:386-94.
49. Kakuta T, Currier JW, Haudenshild CC, Rayan TJ, Faxon DP. Differences in compensatory vessel enlargement, not intimal formation, account for restenosis after angioplasty in the hypercholesterolemic rabbit model. Circulation 1994; 89:2809-15.
50. Losordo DW, Rosenfield K, Kaufman J, Peiczek A, Isner JM. Focal compensatory enlargement of human arteries in response to progressive atherosclerosis. Circulation 1994; 89:2570-7.
51. Anderson HR, Maeng M, Thorwest M, Falk E. Constrictive vascular remodeling rather than neointima formation explains luminal narrowing after deep vessel wall injury: insights from a new porcine coronary stenosis model. Circulation 1995;92:S346.
52. Shi Y, Pieniek M, Fard A, O'Brien JE, Mannion JD, Zalewski A. Adventitial remodeling after coronary arterial injury. Circulation 1996;93:340-8.
53. Dzau VJ, Gibbons GH. Vascular remodeling and restenosis problem. J Cardiovasc Pharmacol 1993;21:S1-S5.
54. Pels K, Labinaz M, Hoffert C, O'Brien ER. Adventitial angiogenesis early after coronary angioplasty: Correlation with arterial remodeling. Arterioscler Thromb Vasc Biol 1999;19:229-38.